Preprints of the 18th IFAC World Congress
Milano (Italy) August 28 - September 2, 2011

Fault Detection and Isolation of a Real Wind Turbine using LPV Observers

Pep Lluís Negre * **Vicenç Puig** ** **Isaac Pineda** *

* *Alstom Wind S.L.U. - Innovation & Reliability,*
Roc Boronat, 78, 08005 Barcelona, Spain,
(e-mail: josep-lluis.negre-carrasco,isaac.pineda-amo@power.alstom.com).
** *Advanced Control Systems Group - Universitat Politècnica de Catalunya,*
Rambla Sant Nebridi, 10, 08222 Terrassa, Spain
(e-mail: vicenc.puig@upc.edu)

Abstract: The purpose of this paper is to design a Fault Detection and Isolation (FDI) system based on LPV observers with application to a real wind turbine. The LPV observer is used to generate an adaptive threshold to enhance the robustness of the fault detection test. Real field data and system identification techniques are used to identify the nominal model as well as its uncertainty. Since wind turbines are highly non-linear systems when operating in their whole range of operation, a Linear Parameter Varying (LPV) model is used. Finally, fault isolation is based on an algorithm that uses the residual fault sensitivity. Several fault scenarios are used to show the performance of the proposed approach.

Keywords: Fault detection, fault isolation, wind turbines, linear parameter varying systems, model error modelling.

1. INTRODUCTION

The future of wind energy passes through the installation of offshore wind farms. In such locations a non-planned maintenance is very costly. Therefore, a fault-tolerant control system that is able to maintain the wind turbine connected after the occurrence of certain faults can avoid major economic losses (Sloth et al., 2010). A first step towards the implementation of a fault-tolerant system is to implement a Fault Detection and Isolation (FDI) that is able to detect, isolate, and if possible to estimate the fault (Isermann, 2006). The problem of model-based fault diagnosis in wind turbines has just been recently addressed mainly motivated because of importance of this technology for generating electricity is gained in many countries. So far, revising the literature, methods raging from Kalman filters (Wei et al., 2009), observers (Odgaard et al., 2009b) or parity equations (Dobrila and Stefansen, 2007) have been already suggested as possible model-based techniques for fault diagnosis of wind turbines

To use any model-based technique it is necessary to obtain a model of the wind turbine. Since most of the techniques available in the literature utilize linear models, the more straightforward approach is to model the wind turbine in this way. However, a linear model will only be able to represent the non-linear wind turbine behaviour around a given operating point. To build a model that is valid along the whole operating range a Linear Parameter Varying (LPV) model will be used. Because the effectiveness of the FDI algorithm relies in its concordance with the reality, the plant model will be constructed using real faultless wind turbine data using system identification methods. Usually, the field data is presented in time series of 10 or 20 minutes. The low recording time causes that it is not possible to get the entire wind speed range (from 3m/s to 25m/s) in a single time series. Therefore, the form of the field data only allows the identification of the system in one wind speed operating point (the mean wind speed for each time series). Thus, several models have to be identified around single points along the full operation range as shown in Fig. 1.

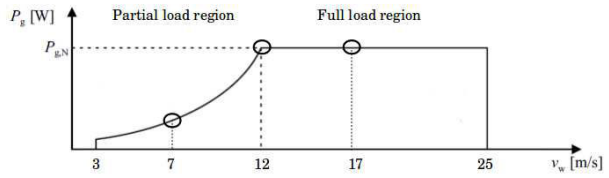

Fig. 1. Power curve range with three possible operating points separated 5m/s between them.

The innovation of this paper is to present the application of a new fault detection and isolation method for nonlinear systems that can be described as LPV models to a wind turbine. The fault detection methodology is based on comparing on-line the real system behavior of the monitored system obtained by means of sensors with the estimated behavior using an *LPV interval observer*. In the case of a significant discrepancy (residual) is detected between the LPV model and the measurements obtained by the sensors, the existence of a fault is assumed. Due to the effect of the uncertain parameters, the outputs of LPV models are bounded by an interval to avoid false alarms in the detection module. Analyzing in real-time how the faults affect to the residuals using the residual fault sensitivity, it is possible, to isolate the fault, and even in some cases it is also possible to determine its magnitude.

In this paper, the proposed model-based FDI approach for wind turbines is applied to a commercial variable-speed, variable-pitch 3MW wind turbine of Alstom Wind S.L.U., named ECO100 (see Figure 2). This machine follows the standard of Danish concept: horizontal axis using a three bladed rotor design with an active yaw system keeping the rotor always

Fig. 2. Alstom ECO100 wind turbine.

oriented upwind. The ECO100 is II-A class IEC/EN-61400-1 with an ideal mean annual wind speed of 8.5m/s and the wind speeds cut-in and cut-off are respectively 3m/s and 25m/s (see Figure 1). The rotor velocity can vary between 7.94 - 14.3 r.p.m. and it has a swept area of 7980m^2. The tower is an hybrid 90m of height with the first 10m of concrete and the rest of steel. Alstom Wind S.L.U. has provided a non-linear simulation model and real field data of ECO100 wind turbine that will be used in the stages of modelling and result validation. These data come from a big set of sensors installed along the wind turbine to collect time-domain measurements from the most important components.

The structure of the paper is the following: In Section 2, the set of faults that will be considered are presented, as well as an overview of the FDI approach that is going to be used. Section 3 presents the proposed robust fault detection methodology based on interval observers. Section 4 introduces the fault isolation algorithm based on the residual fault sensitivities. Then, Section 5 presents the wind turbine case study and the application of the proposed FDI methods. Finally, section 6 gives the main conclusions.

2. WIND TURBINE FAULTS

As in any FDI system, the set of faults to be detected and isolated should be pre-established. With this aim, the set of wind turbine faults that cause the major economic losses (in statistical terms) should be the ones that the FDI system should be designed for. One relevant information available about wind turbine fault statistics is the technical report published by Up-Wind in 2009 (Faulstich and Hahn, 2009) that analyses the faults in the main wind turbine components and related with the different machine typologies. This report indicates that the electrical subsystems fail more often than the mechanical ones, while mechanical subassemblies experience longer downtimes after the failure. But, it is interesting to note that, by examining this failure database, the components of the electrical and control systems fails more often than 2 years and half. In opposite, for example, a failure in the gearbox occurs only every 19 years (see Fig. 3). Similar results were obtained in the study of Ribrant and Bertling (2006) where a statistical analysis about wind turbine failures was done with data of Sweden, Finland and Germany wind companies.

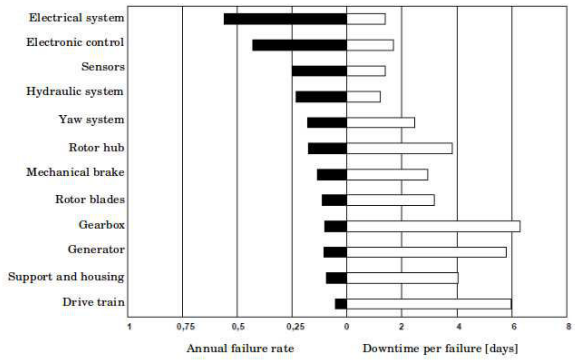

Fig. 3. Reliability statistics for main wind turbine systems.

Analysing these reports, it is clear that the control system is one of those responsible for the greatest number of failures in wind turbines. The sensors are one of the most important parts of the control system since the control actions are directly related to input reference sensors. Thus, it is very reasonable designing a FDI system that takes into account the faults in the sensors to prevent the control malfunctions. Besides the two control actuators governing the *Generator torque* and the *Blade pitch angle* are also susceptible to faults. The faults in actuators can be easily mitigated by fault-tolerant control techniques. Therefore, it is reasonable to include these components in the list of considered faults (Table 1). In (Odgaard et al., 2009a), a benchmark for FDI of wind turbines have been already proposed that also mainly focus in the type of faults addressed in this paper.

Fault	Signal name	Signal type
f_1	Electrical power	sensor
f_2	Generator speed	sensor
f_3	Generator torque	actuator
f_4	Blade pitch angle	actuator
f_5	Wind speed	sensor

Table 1. List of considered faults

3. FAULT DETECTION USING LPV INTERVAL OBSERVERS

3.1 LPV representation

Let us consider that the nonlinear system (in our case the wind turbine) to be monitored can be described by the following LPV representation:

$$\begin{aligned} x(k+1) &= A(\tilde{\vartheta}_k)x(k) + B(\tilde{\vartheta}_k)u_0(k) + F_a(\tilde{\vartheta}_k)f_a(k) \\ y(k) &= C(\tilde{\vartheta}_k)x(k) + D(\tilde{\vartheta}_k)u_0(k) + F_y(\tilde{\vartheta}_k)f_y(k) \end{aligned} \quad (1)$$

where $u_0(t) \in \Re^{n_u}$ is the real system input, $y(t) \in \Re^{n_y}$ is the system output, $x(t) \in \Re^{n_x}$ is the state-space vector, $f_a(t) \in \Re^{n_u}$ and $f_y(t) \in \Re^{n_y}$ represents faults in the actuators and system output sensors, respectively. $\tilde{\vartheta}_k := \vartheta(k)$ is the system vector of time-varying parameters of dimension n_ϑ that change with the operating point scheduled by some measured system variables p_k $(p_k := p(k))$ that can be estimated using some known function: $\vartheta_k = f(p_k)$. However, there is still some uncertainty in the estimated values that can be bounded by:

$$\Theta_k = \{\vartheta_k \in \Re^{n_\vartheta} \mid \underline{\vartheta_k} \leq \vartheta_k \leq \overline{\vartheta_k}\}, \quad \vartheta_k = f(p_k) \quad (2)$$

This set represents the uncertainty about the exact knowledge of real system parameters $\tilde{\vartheta}_k$.

The system (1) describes a model parametrized by a scheduling variable denoted by p_k. In this paper, the kind of LPV system considered are those whose parameters vary affinely in a polytope (Apkarian et al., 1995). In particular, the state-space matrices range in a polytope of matrices defined as the convex hull of a finite number of matrices N. That is,

$$\begin{pmatrix} A(\tilde{\vartheta}_k) & B(\tilde{\vartheta}_k) \\ C(\tilde{\vartheta}_k) & D(\tilde{\vartheta}_k) \end{pmatrix} \in Co\left\{ \begin{pmatrix} A_j(\vartheta^j) & B_j(\vartheta^j) \\ C_j(\vartheta^j) & D_j(\vartheta^j) \end{pmatrix} \right\}$$
$$:= \sum_{j=1}^{N} \alpha_j(p_k) \begin{pmatrix} A_j(\vartheta^j) & B_j(\vartheta^j) \\ C_j(\vartheta^j) & D_j(\vartheta^j) \end{pmatrix}, \quad (3)$$

with $\alpha_j(p_k) \geq 0$, $\sum_{j=1}^{N} \alpha_j(p_k) = 1$ and $\vartheta^j = f(p^j)$ is the vector of uncertain parameters of j^{th} model where each j^{th} model is called a vertex system and it is assumed according property (2) that: $\vartheta^j \in [\underline{\vartheta^j},\ \overline{\vartheta^j}]$.

Consequently, the LPV system (1) can be expressed as follows:

$$\begin{aligned} x(k+1) &= \textstyle\sum_{j=1}^{N} \alpha^j(p_k) \left[A_j(\vartheta^j)x(k) + B_j(\vartheta^j)u_0(k)\right] \\ y(k) &= \textstyle\sum_{j=1}^{N} \alpha^j(p_k) \left[C_j(\vartheta^j)x(k) + D_j(\vartheta^j)u_0(k)\right] \end{aligned} \quad (4)$$

Here A_j, B_j, C_j and D_j are the state space matrices defined for j^{th} model. Notice that, the state space matrices of system (1) are equivalent to the interpolation between LTI models, for example: $A(\tilde{\vartheta_k}) = \sum_{j=1}^{N} \alpha^j(p_k) A_j(\vartheta^j)$.

The polytopic system is scheduled through functions $\alpha^j(p_k)$, $\forall\ j \in [1, \ldots, N]$ that lie in a convex set

$$\Psi = \Big\{ \alpha^j(p_k) \in \mathbb{R}^N, \alpha(p_k) = \left[\alpha^1(p_k), \ldots, \alpha^N(p_k)\right]^T,$$
$$\alpha^j(p_k) \geq 0,\ \forall j,\ \sum_{j=1}^{N} \alpha^j(p_k) = 1 \Big\}. \quad (5)$$

3.2 LPV Interval Observer

The system described by (1) is monitored using a LPV interval observer with Luenberger structure considering parameter uncertainty given by $\vartheta^j \in [\underline{\vartheta^j},\ \overline{\vartheta^j}]$. In the following, we consider only strictly proper systems such that $D = 0$. Consequently, the LPV interval observer can be written by extending the representation of Meseguer et al. (2006) for LTI models as:

$$\begin{aligned} \hat{x}(k+1) &= \sum_{j=1}^{N} \alpha^j(p_k) \left[A_{0,j}(\vartheta^j)\hat{x}(k) + B_j(\vartheta^j)u(k) + L_j y(k)\right] \\ \hat{y}(k) &= \sum_{j=1}^{N} \alpha^j(p_k) \left[C_j(\vartheta^j)\hat{x}(k)\right] \end{aligned} \quad (6)$$

where $A_{0,j}(\vartheta^j) = A_j(\vartheta^j) - L_j C_j(\vartheta^j)$, $u(k)$ is the measured system input vector, $\hat{x}(k)$ is the estimated system state vector, $\hat{y}(k)$ is the estimated system output vector and L_j is the observer gain that has to be designed in order to stabilize the observer given by (6) for all $\vartheta^j \in [\underline{\vartheta}^j, \overline{\vartheta}^j]$. Each observer gain matrix $L_j \in \Re^{n_x \times n_y}$ is designed to stabilize each vertex j^{th} and to guarantee a desired performance ($A_{0,j}$) regarding fault detection for $\vartheta^j \in [\underline{\vartheta^j},\ \overline{\vartheta^j}]$ (Chilali and Gahinet, 1996).

3.3 Observer input/output form

The system in (1) can be expressed in input-output form using the shift operator q^{-1} and assuming zero initial conditions as follows:

$$y(k) = y_0(k) + G_{f_a}(q^{-1}, \tilde{\vartheta}_k) f_a(k) + G_{f_y}(q^{-1}, \tilde{\vartheta}_k) f_y(k) \quad (7)$$

where:

$$y_0(k) = G_u(q^{-1}, \tilde{\vartheta}_k) u_0(k) \quad (8)$$
$$G_u(q^{-1}, \tilde{\vartheta}_k) = C(\tilde{\vartheta}_k)(qI - A(\tilde{\vartheta}_k))^{-1} B(\tilde{\vartheta}_k) + D(\tilde{\vartheta}_k) \quad (9)$$
$$G_{f_a}(q^{-1}, \tilde{\vartheta}_k) = C(\tilde{\vartheta}_k)(qI - A(\tilde{\vartheta}_k))^{-1} F_a(\tilde{\vartheta}_k) \quad (10)$$
$$G_{f_y}(q^{-1}, \tilde{\vartheta}_k) = F_y(\tilde{\vartheta}_k) \quad (11)$$

Alternatively, the observer described by Eq. (6) can be expressed in input-output form by [1] :

$$\hat{y}(k) = \sum_{j=1}^{N} \alpha^j(p_k) \left[G^j(q^{-1}, \vartheta^j)u(k) + H^j(q^{-1}, \vartheta^j)y(k)\right] \quad (12)$$

where:

$$G^j(q^{-1}, \vartheta^j) = C_j(\vartheta^j)(qI - A_{0,j}(\vartheta^j))^{-1} B_j(\vartheta^j) \quad (13)$$
$$H^j(q^{-1}, \vartheta^j) = C_j(\vartheta^j)(qI - A_{0,j}(\vartheta^j))^{-1} L_j \quad (14)$$

The effect of the uncertain parameters ϑ_k on the observer temporal response $\hat{y}(k, \vartheta_k)$ can be bounded using an interval satisfying [2] :

$$\hat{y}(k) \in \left[\underline{\hat{y}}(k), \overline{\hat{y}}(k)\right] \quad (15)$$

in a non-faulty case. Such interval is computed independently for each output (neglecting couplings between outputs):

$$\underline{\hat{y}}(k) = \min_{\vartheta_k \in \Theta} \left\{ \sum_{j=1}^{N} \alpha^j(p_k) \left[G^j(q^{-1}, \vartheta^j)u(k) + H^j(q^{-1}, \vartheta^j)y(k)\right] \right\}$$
$$\overline{\hat{y}}(k) = \max_{\vartheta_k \in \Theta} \left\{ \sum_{j=1}^{N} \alpha^j(p_k) \left[G^j(q^{-1}, \vartheta^j)u(k) + H^j(q^{-1}, \vartheta^j)y(k)\right] \right\}$$

subject to the observer equations given by (6). Such interval can be computed using the algorithm based on numerical optimization presented in Puig et al. (2005).

3.4 Adaptive thresholding

Fault detection is based on generating a nominal residual comparing the measurements of physical variables $y(k)$ of the process with their estimation $\hat{y}(k)$ provided by the associated system model:

$$r(k) = y(k) - \hat{y}(k) \quad (16)$$

where $r(k) \in \Re^{n_y}$ is the residual set and $\hat{y}(k)$ is the prediction obtained using the nominal LPV model. According to Gertler (1998), the computational form of the residual generator, obtained using (12), is:

$$r(k) = \sum_{j=1}^{N} \alpha^j(p_k) \left[-G^j(q^{-1}, \vartheta^j)u(k) + \left(I - H^j(q^{-1}, \vartheta^j)\right) y(k)\right] \quad (17)$$

Alternatively, the residual given by (17) can be also expressed in terms of the effects caused by faults using its internal or unknown-input-effect form (Gertler, 1998). This form, obtained combining (7), (12) and (16), is expressed as:

$$r(k) = r_0(k) + \sum_{j=1}^{N} \alpha^j(p_k) \left[\left(I - H^j(q^{-1}, \vartheta^j)\right) \left(G^j_{f_y}(q^{-1}, \vartheta^j) f_y(k) + G^j_{f_a}(q^{-1}, \vartheta^j) f_a(k)\right)\right] \quad (18)$$

where

[1] In the following, for simplicity and with abuse of notation, transfer functions are used for LPV systems, although computations are performed entirely using the state space representation: $G^{(j)} \triangleq \left[\begin{array}{c|c} A_0^{(j)}(\vartheta^j) & B^{(j)}(\vartheta^j) \\ \hline C^{(j)}(\vartheta^j) & 0 \end{array}\right]$

[2] In the remainder of the paper, interval bounds for vector variables should be considered component wise.

$$\sum_{j=1}^{N} \alpha^j(p_k) G^j_{fy}(q^{-1},\vartheta^j) = G_{fy}(q^{-1},\tilde{\vartheta_k})$$
$$\sum_{j=1}^{N} \alpha^j(p_k) G^j_{fa}(q^{-1},\vartheta^j) = G_{fa}(q^{-1},\tilde{\vartheta_k})$$

$$r_0(k) = \sum_{j=1}^{N} \alpha^j(p_k) \left[-G^j(q^{-1},\vartheta^j)u(k) + \left(I - H^j(q^{-1},\vartheta^j)\right) y_0(k)\right] \tag{19}$$

Notice that, the expression (19) represents the non-faulty residual. Comparing (17) and (19), it should be noticed that both $r_0(k)$ and $r(k)$ are affected in the same way by the observation gain L.

When considering model uncertainty, the residual generated by (16) will not be zero, even in a non-faulty scenario. To cope with the parameter uncertainty effect a passive robust approach based on adaptive thresholding can be used (Horak, 1988). Thus, using this passive approach, the effect of parameter uncertainty in the residual $r(k)$ (associated to each system output $y(k)$) is bounded by the interval:

$$r(k) \in [\underline{r}(k), \overline{r}(k)] \tag{20}$$

where:

$$\underline{r}(k) = \underline{\hat{y}}(k) - \hat{y}(k) \text{ and } \overline{r}(k) = \overline{\hat{y}}(k) - \hat{y}(k) \tag{21}$$

being $\hat{y}(k)$ the nominal predicted output, $\underline{\hat{y}}(k)$ and $\overline{\hat{y}}(k)$ the bounds of the predicted output (15) using observer (6). The residual generated by (21) can be expressed in input-output form using (12) as:

$$\underline{r}(k) = \min_{\theta\in\Theta} \left\{ \sum_{j=1}^{N} \alpha^j(p_k) \left[\Delta G^j(q^{-1},\vartheta^j)u(k) + \Delta H^j(q^{-1},\vartheta^j)y(k)\right] \right\} \tag{22}$$

$$\overline{r}(k) = \max_{\theta\in\Theta} \left\{ \sum_{j=1}^{N} \alpha^j(p_k) \left[\Delta G^j(q^{-1},\vartheta^j)u(k) + \Delta H^j(q^{-1},\vartheta^j)y(k)\right] \right\} \tag{23}$$

where:

$$\begin{aligned} \Delta G^j(q^{-1},\vartheta^j) &= G^j(q^{-1},\vartheta^j) - G^j(q^{-1},\vartheta^j_0) \\ \Delta H^j(q^{-1},\vartheta^j) &= H^j(q^{-1},\vartheta^j) - H^j(q^{-1},\vartheta^j_0) \end{aligned}$$

being ϑ^j_0 the nominal parameters.

Then, a fault is indicated if the residuals do not satisfy the relation given by (20), or alternatively, if the measurement is not inside the interval of predicted outputs given by (16)-(16).

Fig. 4 summarizes the robust fault detection scheme proposed. The main signals that appear in the picture are the following: the controller actions (u), the measured outputs (y), the estimated outputs ($\hat{y}$), the residual (r), the observer correction (c) and the fault (f). By examining the *residual generation* block, one can see that, in addition to the nominal model, includes an observer scheme. The nominal model is used to estimate the outputs that more closely fits the current wind turbine outputs. The observer is placed in order to avoid drifting between the estimated and measured outputs that would cause erroneous fault detection. On the other hand, *residual evaluation* part is responsible for generating the threshold taking into account the model uncertainty. These limits take into account the uncertainty in the modelling stage (by using a model of the error) and make the FDI system robust.

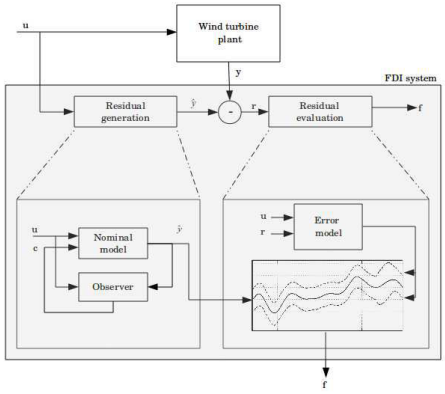

Fig. 4. Complete model-based FDI scheme designed in this research.

4. FAULT ISOLATION USING LPV FAULT SENSITIVITIES

4.1 Fault signature matrix

Fault isolation consists in identifying the faults affecting the system. It is carried out on the basis of fault signatures, (generated by the detection module) and its relation with all the considered faults, $f(k)$=$\{f_a(k), f_y(k)\}$. Robust residual evaluation presented in Section 3.4 allows obtaining a set of *fault signatures* $\phi(k) = [\phi_1(k), \phi_2(k), \ldots, \phi_{ny}(k)]$, where each fault indicator is given by:

$$\phi_i(k) = \begin{cases} 0 \text{ if } r(k) \notin [\underline{r}(k), \overline{r}(k)] \\ 1 \text{ if } r(k) \in [\underline{r}(k), \overline{r}(k)] \end{cases} \tag{24}$$

The standard FDI fault isolation method is based on exploiting the relation defined on the Cartesian product of the sets of considered faults:

$$FSM \subset \phi \times f, \tag{25}$$

where *FSM* is the theoretical fault signature matrix (Gertler, 1998). One element of such matrix $FSM_{i\ell}$ will be equal to one, if the fault $f_\ell(k)$ is affected by the residual $r_i(k)$. In this case, the value of the fault indicator $\phi_i(k)$ must be equal to one when the fault appears in the monitored system. Otherwise, the element $FSM_{i\ell}$ will be zero.

In this work, it is proposed to use of information provided by the *fault residual sensitivity* in the design of the diagnosis system in order to increase fault isolability.

4.2 LPV Fault residual sensitivity

In general, the occurrence of a fault signal can be caused by different faults. Therefore what allows distinguishing one fault from the others are the fault signal dynamic properties that should be different for each different fault. According to (Gertler, 1998), these theoretical dynamic properties are described by the *residual fault sensitivity* that can be expressed as follows:

$$S_f = \frac{\partial r}{\partial f} \tag{26}$$

which is a transfer function that describes the effect on the residual, r, of a given fault f. The expression of residual sensitivity is obtained using the residual internal form given by (18). Thus, the sensitivity changes with the operating point parametrized by scheduling variable p_k as the LPV system (1).

The residual (18) can be re-written as follows:

$$r(k) = r_0(k) + S_{f_y}(q^{-1}, \tilde{\vartheta}_k) f_y(k) + S_{f_a}(q^{-1}, \tilde{\vartheta}_k) f_a(k) \quad (27)$$

where S_{f_y} is the sensitivity of the output sensor fault and S_{f_a} is the sensitivity of the actuator fault.

LPV Residual sensitivity of an output sensor fault

Analyzing the residual internal form given by (27), and considering the fault residual sensitivity definition given by (26), the residual sensitivity for the case of a output sensor fault f_y is given by a matrix S_{f_y} of dimension $n_y \times n_y$ whose expression is:

$$S_{f_y}(q^{-1}, \tilde{\vartheta}_k) = \sum_{j=1}^{N} \alpha^j(p_k) \left[\left(I - H^j(q^{-1}, \vartheta^j) \right) G^j_{fy}(q^{-1}, \vartheta^j) \right] = \begin{bmatrix} S_{fy_{1,1}}(q^{-1}, \tilde{\vartheta}_k) & \cdots & S_{fy_{1,n_y}}(q^{-1}, \tilde{\vartheta}_k) \\ \vdots & \ddots & \vdots \\ S_{fy_{n_y,1}}(q^{-1}, \tilde{\vartheta}_k) & \cdots & S_{fy_{n_y,n_y}}(q^{-1}, \tilde{\vartheta}_k) \end{bmatrix} \quad (28)$$

where the element of this matrix located at the i^{th}-row and in the ℓ^{th}-column. $S_{fy_{i,\ell}}$ describes the sensitivity of the residual $r_i(k)$ regarding the fault $f_{y_\ell}(k)$ affecting the output sensor.

LPV Residual sensitivity of an actuator fault

Applying the analysis procedure used in the output sensor case, the residual sensitivity of an actuator fault f_a is given by a matrix S_{fa} of dimension $n_y \times n_u$:

$$S_{f_a}(q^{-1}, \tilde{\vartheta}_k) = \sum_{j=1}^{N} \alpha^j(p_k) \left[\left(I - H^j(q^{-1}, \vartheta^j) \right) G^j_{fa}(q^{-1}, \vartheta^j) \right] = \begin{bmatrix} S_{fa_{1,1}}(q^{-1}, \tilde{\vartheta}_k) & \cdots & S_{fa_{1,n_u}}(q^{-1}, \tilde{\vartheta}_k) \\ \vdots & \ddots & \vdots \\ S_{fa_{n_y,1}}(q^{-1}, \tilde{\vartheta}_k) & \cdots & S_{fa_{n_y,n_u}}(q^{-1}, \tilde{\vartheta}_k) \end{bmatrix} \quad (29)$$

where each row of this matrix is related to one component of the residual vector $r(k) = \{r_i(k) : i = 1, 2, \ldots, n_y\}$ while each column is related to one component of the actuator fault vector $f_a = \{f_{a,\ell} : \ell = 1, 2, \ldots, n_u\}$.

4.3 Fault isolation algorithm

Figure 5 shows the scheme of the fault diagnosis algorithm proposed in this paper. The detection module has been alredy explained in Section 3. The result of this module applied to the residual $r(k)$ produces an *observed fault signature* $\phi(k)$. The observed fault signature is then supplied to the fault isolation module that will try to isolate the fault so that a fault diagnosis can be produced.

In this paper, a new fault isolation approach is proposed that makes use of the fault estimation provided the residual fault sensitivity (26). More precisely, assuming that $\left(S_f(q^{-1}, \tilde{\vartheta}_k) \right)^{-1}$ exists [3], the expression of the fault estimation is given by:

$$\hat{f}_{\varrho,\ell}(k) = \left(S_{f_{\varrho,\ell}}(q^{-1}, \tilde{\vartheta}_k) \right)^{-1} r_i(k) \quad (30)$$

where $i \in [1, \ldots, n_y]$ and being $\hat{f}_{\varrho,\ell} = \left\{ \hat{f}_{y,\ell}, \hat{f}_{a,\ell} \right\}$, $\forall\ \ell \in [1, \ldots, n_y, 1, \ldots, n_u]$. This relation considers the influence of each fault $f(k)$ on the each residual $r(k)$. Notice that, the sensitivity expression changes with the operating point and consequently the fault estimation is parametrized by scheduling variable p_k.

[3] If $\left(S_f(q^{-1}, \tilde{\vartheta}_k) \right)^{-1}$ is non-square and can be tackled using the left pseudo-inverse

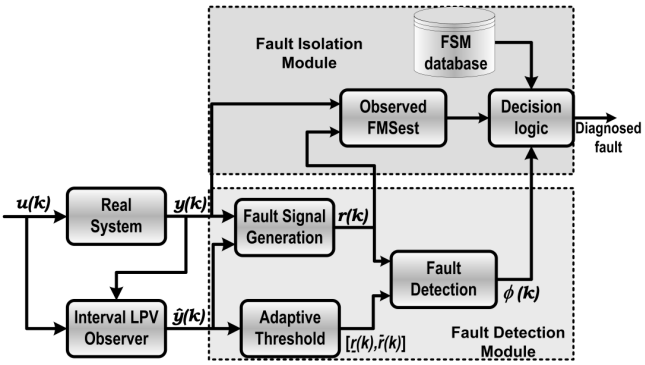

Fig. 5. Block diagram of the fault diagnosis system.

Using the fault estimation (30), a new *FSM* matrix (called *fault signature matrix FSMest*) can be defined as shown in Table 2. This fault signature matrix is evaluated at every time instant.

$\hat{f}_{\varrho,\ell}$	$f_{y,1}$	$\cdots$	f_{y,n_y}	$f_{a,1}$	$\cdots$	f_{a,n_u}
$r_1(k)$	$\hat{f}_{r_1 f_{y,1}}$	$\cdots$	$\hat{f}_{r_1 f_{y,n_y}}$	$\hat{f}_{r_1 f_{a,1}}$	$\cdots$	$\hat{f}_{r_1 f_{a,n_u}}$
$r_2(k)$	$\hat{f}_{r_2 f_{y,1}}$	$\cdots$	$\hat{f}_{r_2 f_{y,n_y}}$	$\hat{f}_{r_2 f_{a,1}}$	$\cdots$	$\hat{f}_{r_2 f_{a,n_u}}$
$\vdots$	$\vdots$	$\ddots$	$\vdots$	$\vdots$	$\ddots$	$\vdots$
$r_{n_y}(k)$	$\hat{f}_{r_{n_y} f_{y,1}}$	$\cdots$	$\hat{f}_{r_{n_y} f_{y,n_y}}$	$\hat{f}_{r_{n_y} f_{a,1}}$	$\cdots$	$\hat{f}_{r_{n_y} f_{a,n_u}}$

Table 2. Fault signature matrix based on the fault estimation (*FSMest*) with respect to $r_i(k)$

Each fault hypothesis corresponds to each ℓ^{th}-column of *FSMest* matrix of Table 2. The fault hypothesis corresponding to ℓ^{th}-column is accepted if all the fault estimation values are equal. More precisely, assuming that the system is just affected by one fault $f(k)$ at a time t_0, the isolation process is done by finding the fault that presents a fault estimation with a minimum distance with respect to the average of fault estimation hypothesis being postulated as a diagnosed fault:

$$\min \left\{ d_{f_{y,1}}, \ldots, d_{y,n_y}, d_{f_{a,1}}, \ldots, d_{a,n_u} \right\} \quad (31)$$

where the distance is calculated using the Euclidean distance between vectors:

$$d_{f_{\varrho,\ell}} = \sqrt{\left(\hat{f}_{r_1 f_{\varrho,\ell}}(k) - \hat{f}^m_{f_{\varrho,\ell}}(k) \right)^2 + \cdots + \left(\hat{f}_{r_{ny} f_{\varrho,\ell}}(k) - \hat{f}^m_{f_{\varrho,\ell}}(k) \right)^2} \quad (32)$$

where:

$$\hat{f}^m_{f_{\varrho,\ell}}(k) = \frac{\sum_{i=1}^{n_y} \hat{f}_{r_i f_{\varrho,\ell}}(k)}{n_y}$$

for $f_{\varrho,\ell} = \{f_{y,\ell}, f_{a,\ell}\}$, $\forall\ \ell \in [1, \ldots, n_y, 1, \ldots, n_u]$.

Finally, in order to prevent false alarms when the fault signals appears in different time instants, Puig et al. (2005) proposes a solution that consists in not allowing an isolation decision until a prefixed waiting time (T_w) has elapsed from the first fault signal appearance. This time T_w can be calculated from the largest transient time response from non-faulty situation to any faulty situation. The value T_w must be evaluated once the first residual is activated. This interval of time is maximum when the fault is the minimum isolable fault. Such a fault will be determined in the next section.

5. APPLICATION TO A REAL WIND TURBINE

5.1 Wind turbine model for FDI

For FDI purposes the measured variables used for the control of the wind turbine were considered. Fig. 6 illustrates the basic control scheme of the wind turbine Alstom ECO100. The inputs of the plant are the wind speed υ, which can be divided in mean wind speed $\overline{\upsilon}$ and the turbulent part $\widetilde{\upsilon}$, the generator torque reference τ_{ref} and pitch angle reference β_{ref}. On the other hand, the outputs of the plant are the angular generator speed ω and the electrical power P.

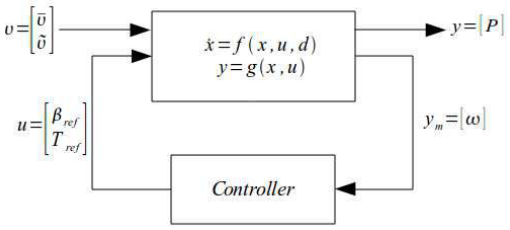

Fig. 6. Control scheme for the ECO100 wind turbine.

The GH Bladed model [4] of the ECO100 wind turbine was delivered by Alstom. This is an encrypted model that does not allow to use the model equations explicitly. However, this model can be used to extract information about the structure of the model to be used when identifying a LPV model for fault detection. GH Bladed allows users to linearize its internal non-linear model at any wind turbine operating point.

The linear model obtained with GH Bladed around a given operating point contains all the dynamics and can be a higher order model (upper than 40 states). Therefore, it is useless to be used for designing a FDI system. These techniques usually require relatively low order models but high accuracy. With this aim, a set of lower models relating each output signal with the considered input signals are obtained using the Hankel model reduction technique (see Figure 7). The order of each model is presented in Table 3.

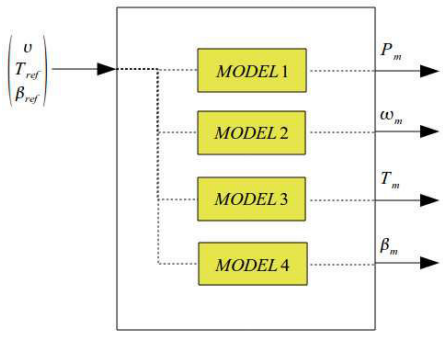

Fig. 7. Bank of models for FDI

Once the structure of the models have been determined, the parameters of the nominal models has been estimated around each considered operating using real data coming from a real ECO100 wind turbine and the MATLAB identification toolbox. Figure 8 shows the result of model prediction for the electrical power output after parameters have been calibrated at different operating points. Once the parameters around each operating point have obtained, the scheduling functions $\tilde{\vartheta}_k = f(p_k)$ for the LPV parameters are approximated by polynomials whose coefficients are estimated following the procedure described in Bamieh and Giarre (2002) using data taken at different operating points $p_k \in [\underline{p}, \overline{p}]$.

[4] GH Bladed is a program for wind turbine modelling highly validated which provides very accurate non-linear simulation models

Model	Output	Order
1	Electrical power	4
2	Generator speed	4
3	Generator torque	2
4	Blade pitch angle	3

Table 3. Order of the FDI models

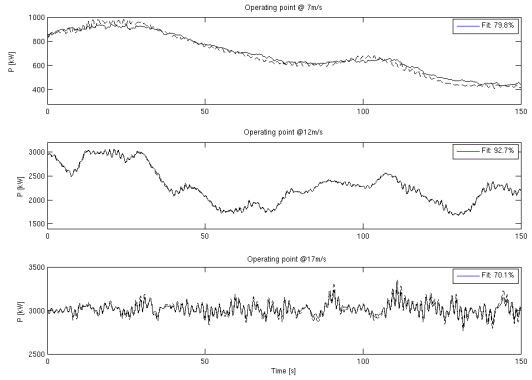

Fig. 8. Electrical power model prediction

5.2 Model error modelling

The uncertainty model around each operating point is obtained by Model Error Modelling (MEM) techniques proposed by Reinelt et al. (2001). The basic idea of MEM is to use the nominal model identified in the previous section (denoted G_0), and a collection of measured field data (y, u) to identify an error model as follows:

(1) Compute the residual $\epsilon = y - G_0 u$.
(2) Consider the "error system", with input u and output ϵ, and identify a model G_e for this system. This is an estimation of the error due to undermodeling, the so-called MEM.

Identification of the MEM from residual data can be seen as a separation between noise and unmodeled dynamics. In fact, G_e is an estimation of the dynamic system ΔG, such that:

$$\epsilon(k) = \Delta G u(k) + e(k) \tag{33}$$

If not knowledge about the structure of this model exists and in the absence of specific suspected non-linearities, it is reasonable to test non-linear neural networks black boxes (Ljung (1999)) to identify the error model. It means that the Eq. (33) can be rewritten as:

$$\epsilon(k) = \widetilde{f}(u(k)) + e(k) \tag{34}$$

where $\widetilde{f}$ is a non-linear function that can be modeled f.e. using a neural network NNFIR model.

Figure 9 shows the prediction provided by nominal and error models once have been calibrated using real data for the electrical power output (Model 1 in Table 3).

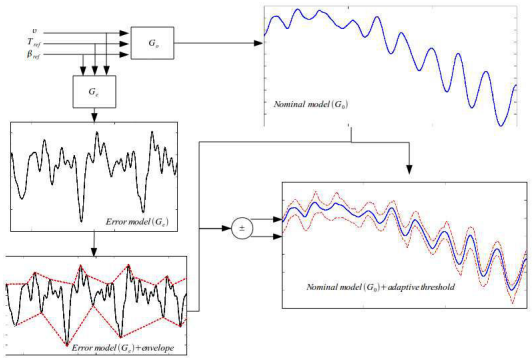

Fig. 9. Prediction provided by nominal and error models

5.3 FDI system design

The methods presented in the previous sections allow the FDI system to detect faults but not to isolate them. There are some faults that can cause the activation of more than one residual as for example in the case of the wind sensor. Since the wind speed is an input of all models in the FDI scheme, a fault in this sensor can cause an activation of all residual signals. There is no way to determine if a fault in such signal will induce a massive residual activation because it depends on the type and magnitude of the fault. The results described in Mesenguer et al. (2010) enables FDI system to identify the source of fault by analysing the residual sensitivities. The Table 4 indicates to the FDI system which is the transfer function that determines the time evolution should have the residual signal for each fault. Then, for example, if there is a fault in the wind speed sensor, the residual of model 1 (with electrical power output) must have the same shape than the indicated by the sensitivity $S_{fu}(q)$.

Fault	Signal name	Signal type	Sensitivity
f_1	Electrical power	output sensor	$S_{fy}(q)$
f_2	Generator speed	output sensor	$S_{fy}(q)$
f_3	Generator torque	actuator	$S_{fa}(q)$
f_4	Blade pitch angle	actuator	$S_{fa}(q)$
f_5	Wind speed	input sensor	$S_{fu}(q)$

Table 4. Sensitivity analysis of each fault according its type.

5.4 Results

Let us consider, for example, an abrupt fault scenario in wind speed input sensor. In such case, the fault was only detected by the residual corresponding to generator speed output sensor (see Figure 10). Without the use of the residual sensitivity analysis, the FDI system would have assigned the fault to generator speed sensor and the reconfiguration action taken by the fault-tolerant control would be wrong. Note that two faults could have affected to the generator speed residual: fault f_2 (generator speed sensor fault) and f_5 (wind speed sensor fault).

Therefore, the corresponding two residual sensitivity functions have to be analysed and shown in Figure 11. In this figure, the time evolution of the residual sensitivity for model 2 with generator speed output is illustrated. The left graph is the fault

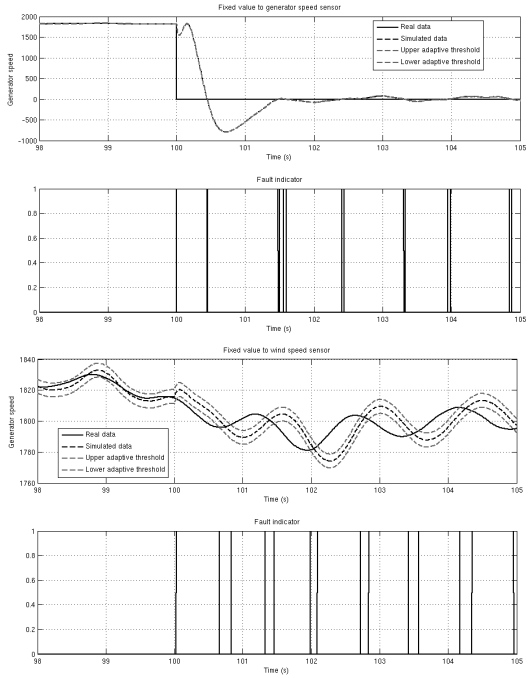

Fig. 10. Fault detection results using model 2 in case of fault f_2 (two upper plots) and f_5 (two lower plots), respectively.

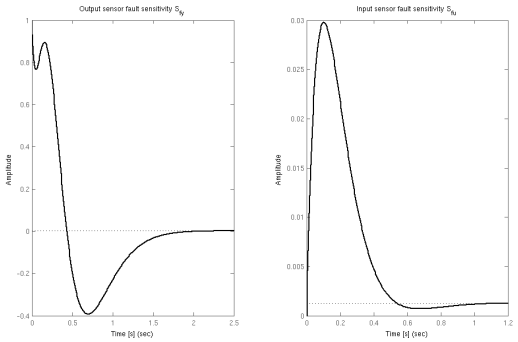

Fig. 11. Time evolution of the residual sensitivity for generator speed.

sensitivity to an output sensor fault, i.e. a fault in the generator speed sensor. The right graph is the fault sensitivity to an input sensor fault, i.e. a fault in the wind speed sensor. Both curves are different, thus the faults are isolable using residual fault sensitivities.

Let us consider now the two possible fault scenarios described in the list above with an abrupt fault (fixed value to 0) in both cases. Figure 10 illustrates the FDI internal signals for the corresponding model when these faults occur. The figure shows the generator speed output sensor fault (abrupt fault) in the top plot, and the wind speed input sensor fault (abrupt fault) in the bottom plot. It is obvious that both scenarios cause different behaviours in the estimated output: when an abrupt fault is done in generator speed output sensor, the estimated output is not able to fit the real faulty measurement. Thus the fault indicator is always active after the fault. When an abrupt fault is given in wind speed input sensor, not only the input of the model is affected because the LPV model uses this signal for the parameter variation. Therefore, after the transient is difficult to determine what happens with the estimated output. However,

the signal time evolution in the transient zone can be analysed in order to find out the fault origin. By examining Figure 11 and Figure 10 it is easy to see that the faults are clearly isolable since the estimated output follows the shape of the corresponding residual sensitivity in the transient. For the case of wind speed input sensor fault, the transient has less amplitude than in the generator speed output sensor fault. This effect is also visible in Figure 11 where the residual sensitivities have different amplitude scale being much lower the one corresponding to wind speed input sensor.

6. CONCLUSIONS

In this paper, a FDI system has been developed for wind turbines. The study is based on a ECO100 model (a variable-speed, variable pitch 3MW real wind turbine) using real data provided by the company Alstom Wind S.L.U. The wind turbine faults considered are chosen based on published statistical studies of wind turbine faults and are related to elements used for the control system that include sensor and actuator faults. Models for FDI have been constructed using system identification methods using real wind turbine field data to achieve the maximum matching with the reality. Additionally, the uncertainty is taken into account to be robust against modelling errors and signal noise. This goal is achieved by using techniques of model error modelling that allow finding a model for the uncertainty. The fault detection has been addressed through LPV interval observers. The fault isolation task has been implemented using the concept of residual fault sensitivities. This concept has been exploited to provide additional information to the relationship between residuals and faults. Moreover, it allows obtaining the possible fault estimation for each residual signal. Additionally the minimum detectable and isolable fault has been presented. This information is important to evaluate the limits of fault diagnosis method. For faults smaller than minimum detectable/isolatable fault, this methodology can not detect or isolate the fault, respectively. Satisfactory results have been obtained in several fault scenarios in the considered wind turbine.

7. ACKNOWLEDGMENTS

This work has been partially funded by the grant CICYT HYFA DPI2008-01996 of Spanish Ministry of Education.

REFERENCES

Apkarian, P., Gahinet, P., and Becker, G. (1995). Self-scheduled H_∞ control of linear parameter-varying systems: a design example. *Automatica*, 31(9):1251 – 1261.

Bamieh, B. and Giarre, L. (2002). Identification of Linear Parameter Varying Models. *International Journal Robust Nonlinear Control*, 2(12):841–853.

Chilali, M. and Gahinet, P. (1996). H_∞ design with pole placement constraints: an LMI approach. *IEEE Transactions on Automatic Control*, 41(3):358–367.

Dobrila, C. and Stefansen, R. (2007). *Fault tolerant wind turbine control*. Master's thesis, Technical University of Denmark, Kgl. Lyngby, Denmark.

Faulstich, S. and Hahn, B. (2009). Comparison of different wind turbine concepts due to their effects on reliability. *Project Upwind*.

Gertler, J. (1998). *Fault Detection and Diagnosis in Engineering Systems*. Marcel Dekker, New York.

Horak, D. T. (1988). Failure detection in dynamic systems with modelling errors. *Journal of Guidance, Control, and Dynamics*, 11(6):508–516.

Isermann, R. (2006). *Fault Diagnosis Systems: An Introduction from Fault Detection to Fault Tolerance*. Springer, New York.

Ljung, L. (1999). Model validation and model error modeling. *Linkopings universitet*.

Meseguer, J., Puig, V., and Escobet, T. (2006). Observer gain effect in linear interval observer-based fault detection. *Sixth IFAC Symposium on Fault Detection, Supervision and Safety of Technical Processes*, 6.

Mesenguer, J., Puig, V., Escoert, T., and Saludes, J. (2010). Observer gain effect in linear interval observer-based fault detection. *Process Control*.

Odgaard, P., Stoustrup, J., and Kinnaert, M. (2009a). Fault tolerant control of wind turbines - a benchmark model. In *7th IFAC Symposium on Fault Detection, Supervision and Safety of Technical Processes (SAFEPROCESS'09)*, Barcelona, Spain.

Odgaard, P. F., Stoustrup, J., Nielsen, R., and Damgaard, C. (2009b). Observer based detection of sensor faults in wind turbines. In *In Proceedings of European Wind Energy Conference 2009*, Marseille, France.

Puig, V., Schmid, F., Quevedo, J., and Pulido, B. (2005). A new fault diagnosis algorithm that improves the integration of fault detection and isolation. *44th IEEE Conference on Decision and Control, and the European Control Conference 2005. Seville, Spain*, pages 3809–3814.

Reinelt, W., Garulli, A., and Ljung, L. (2001). Model error modelling in robust identification. *Linkopings universitet*.

Ribrant, J. and Bertling, L. (2006). Reliability performance and maintenance - a survey of failures in wind power systems. *KTH School of Electrical Engineering*.

Sloth, C., Esbensen, T., and Stoustrup, J. (2010). Active and passive fault-tolerant lpv control of wind turbines. In *In Proceedings of American Control Conference*, Baltimore, USA.

Wei, X., Verhaegen, M., and van den Engelen, T. (2009). Sensor fault diagnosis of wind turbines for fault tolerant. In *In Proceedings of 17th World Congress The International Federation of Automatic Control*, Seoul, South Korea.